Study on the Oriented Recrystallization of Carbon-Coated Polyethylene Oriented Ultrathin Films

Haibo Chang,[†,‡] Qipeng Guo,[§] Deyan Shen,[†] Lin Li,[†] Zhaobin Qiu,[∥] Feng Wang,*[,∥] and Shouke Yan*[,†,∥]

Institute of Chemistry, The Chinese Academy of Science, Beijing 100190, P. R. China, Chemistry and Chemical Engineering College, Henan University, Kaifeng 475001, P. R. China, Centre for Material and Fibre Innovation, Deakin University, Geelong, Victoria 3271, Australia, and State Key Laboratory of Chemical Resource Engineering, Beijing University of Chemical Technology, Beijing 100029, P. R. China

Received: July 27, 2010; Revised Manuscript Received: September 5, 2010

It is confirmed that a layer of vacuum-evaporated carbon on the surface of a preoriented ultrathin polymer film can lead to an oriented recrystallization of the polymer film. This has been attributed to a strong fixing effect of vacuum-evaporated carbon layer on the film surface of the polymer. To study the origin of the strong fixing effect of vacuum-evaporated carbon layer on the polymer films, the melting and recrystallization behaviors of the preoriented ultrathin PE film with a vacuum-evaporated carbon layer were studied by using atomic force microscopy, electron diffraction, Fourier transform infrared spectroscopy, and Raman spectroscopy. We found that there exists some extent of chain orientation of carbon-coated polyethylene (PE) preoriented ultrathin film above its melting temperature. These oriented PE chain sequences act as nucleation sites and induce the oriented recrystallization of preoriented PE film from melt. Raman spectroscopy results suggest that new carbon−carbon bonds between the carbon layer and the oriented PE film are created during the process of vacuum carbon evaporation. As a result, some of the PE chain stems are fixed to the coated carbon substrate via covalent bond. Such a bonding has retarded the relaxation of the PE chains at the spot and, therefore, preserves the original orientation of the PE stems at high temperature, which in turn derives the recrystallization of the PE chains in an oriented structure.

Introduction

Replica technique has been frequently used to record the surface topology of bulk materials for fine structure observation by using transmission electron microscope (TEM).[1−6] More than 40 years ago, in an approach to dissolve the polyethylene (PE) from its carbon-coated single crystals for getting detached replicas, Bassett and his co-workers found that the dissolution temperature of PE in xylene increasesd remarkably by vacuum evaporating a thin layer of carbon on the single crystal fold surface.[4−6] They reported that the xylene has no dissolution effect on the carbon-coated PE single crystals at temperatures below 85 °C (or even 95 °C for the thicker lamellar single crystals). One can peel the PE single crystals off the carbon layer completely only when dissolving the carbon-coated PE single crystals in xylene at temperatures above 105 °C. In the temperature range from 95 to 105 °C, the single crystal layers which are not in contact with the carbon coating can be removed, while a monolayer PE single crystal remains on the carbon coating. Their results demonstrated the fixing effect of vacuum-evaporated carbon toward PE single crystals. This effect has been confirmed by recent studies on the melt recrystallization behavior of carbon-coated PE single crystals.[7,8] Both Yang et al.[7] and Kawaguchi et al.[8] confirmed that the carbon-coated PE single crystals can retain their single crystal structure after complete melting at temperatures as high as 200 °C and subsequent recrystallization. On the other hand, in our previous studies, we have vacuum deposited carbon on the side surfaces of edge-on lamellae instead of flat-on single crystal fold surface.[9−13] Dissolution test showed that the PE could not be completely removed from the carbon coating by xylene at 120 °C. Melt recrystallization experiments indicated that the chain orientation of a series of carbon-decorated preoriented polymer films could be maintained after complete melting and subsequent recrystallization. Moreover, the crystalline structure could be affected by the carbon coating. For example, a phase transition of PVDF from its oriented α phase to an oriented β phase has been realized during melt recrystallization.[9] This may be of great importance since micropatterned thin polymer films with periodic or well-defined oriented and nonoriented structures, even with different crystalline structures, can be easily prepared through selective carbon coating with the help of a mask and subsequent melt recrystallization.[13]

The above-described phenomena displayed the effect of vacuum-evaporated carbon film on the recrystallization behavior of the semicrystalline polymer films. It is suggested that the carbon layer has fixed the surface monolayer macromolecular chains of the polymer films and therefore prevents the extended macromolecular chain stems in crystalline phase from relaxation during high-temperature thermal treatment. These extended or at least relatively extended chain stems then act as the nucleation sites during the recrystallization process and induce the oriented regrowth of the polymer melts. There is, however, no direct experimental evidence of it. Also the mechanism of the fixing effect of the vacuum-deposited carbon layer on the polymer

* To whom correspondence should be addressed. E-mail: skyan@mail.buct.edu.cn (S.Y.); wangf@mail.buct.edu.cn (F.W.). Tel.: +86-10-64455928. Fax: +86-10-64455928.
† The Chinese Academy of Science.
‡ Henan University.
§ Deakin University.
∥ Beijing University of Chemical Technology.

10.1021/jp106995f
Published on Web 09/24/2010

chain stems is not quite clear. Therefore, further studies on this issue are necessary.

It should be pointed out that all of the early investigations on this topic have been focused on the morphological and structural features of the oriented thin polymer films before and after melt recrystallization. Spectroscopy, e.g., infrared and Raman spectroscopy, has been frequently used to follow molecular structure and conformation changes during melting and crystallization processes of semicrystalline polymer.[14−16] They are very sensitive to both chain conformation and molecular environment. Therefore, the melt recrystallization process of the carbon-coated preoriented thin polyethylene films was followed by Fourier transform infrared spectroscopy (FTIR) and Raman spectroscopy. The results shed some more light on the origin of the fixing effect of vacuum-evaporated carbon layer. The purpose of this paper is to present the detailed experimental results and some interesting findings concerning the fixing mechanism of vacuum-evaporated carbon layer on thin polymer films.

Experimental Section

High-density polyethylene (PE), Lupolen 6021DX, was obtained from BASF AG Ludwigshafen, Germany. Uniaxially oriented thin films of PE were prepared according to the melt-drawn technique introduced by Petermann and Gohil.[17] According to this method, a small amount of a 0.5 wt % solution of the PE in xylene was poured and uniformly spread on a preheated glass plate at 125 °C, where the solvent was allowed to evaporate. After evaporation of the solvent, the remaining thin PE melt layer was then drawn up by a motor-driven cylinder with a drawing speed of 20 cm/s, and highly oriented PE ultrathin films of ca. 50 nm in thickness were collected by glass frames. The obtained PE ultrathin films were either single side or double sides coated with thin carbon layers (ca. 5 nm) via vacuum evaporation to get carbon-coated PE melt-drawn films. The obtained carbon-coated PE films were then transferred to copper grids, glass slide, or KBr disk and melt recrystallized at different thermal conditions for different measurements.

For AFM observation, a Nano-Scope III MultiMode AFM (Digital Instruments) was used in this study. Si cantilever tips (TESP) with a resonance frequency of approximately 300 kHz and a spring constant of about 40 N m^{-1} were used. The scan rate varied from 0.5 to 1.0 Hz. The set-point amplitude ratio (rsp) A_{sp}/A_0 was adjusted to 0.7−0.9, where A_{sp} is the set-point amplitude and A_0 is the amplitude of the free oscillation. The set-point ratio and amplitude were chosen such that the surface was tracked while maintaining the necessary contrast in the phase images. The electron diffraction patterns corresponding to the original and recrystallized ultrathin PE films were taken with a Philips CM200 TEM operated at 200 kV.

For IR study, a Bruker Vetex 70 Fourier transform infrared spectrometer equipped with a DTGS detector and a variable temperature cell was used. The carbon-coated melt-drawn PE films covered on slippery KBr plates were used for transmission infrared spectroscopy (TIR) investigation. To testify the orientation of the molecular chains both in crystalline and amorphous regions of the melt-drawn thin PE films, polarized beam parallel and perpendicular to the drawing direction was used. The spectra in the region of 4000−400 cm^{-1} were obtained by averaging 32 scans at a 4 cm^{-1} resolution. For reflection−absorption infrared (RAIR) measurement, the same infrared spectrometer equipped with an MCT detector was used. The incidence angle was set at 83° for the best signal recording. The polarization of the incoming beam was parallel to the plane of incidence (P-polarized).

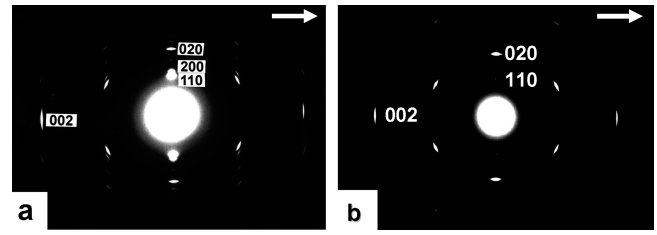

Figure 1. Electron diffraction patterns of carbon-coated ultrathin PE melt-drawn films before and after heat-treatment: (a) as-prepared PE thin film; (b) recrystallized isothermally at 100 °C for 2 h after melting at 150 °C for 10 min. The arrows represent the drawing direction of the thin films during preparation.

Raman spectroscopic measurements were generated using a Renishaw InVia Raman microscope. The excitation lines are 514 nm with a power of 10 mW.

Results and Discussion

We here first present the oriented recrystallization phenomenon of the preoriented PE films. Figure 1 shows the electron diffraction patterns of the as-prepared and melt recrystallized carbon-coated ultrathin PE melt-drawn films. In both electron diffraction patterns, there are sharp and well-defined diffraction spots, which demonstrate a highly oriented structure of the as-prepared and melt-recrystallized carbon-coated ultrathin PE films. All of the diffraction spots in Figure 1a and b have been accounted for by the orthorhombic unit cell with axes $a = 0.74$, $b = 0.494$, and $c = 0.2534$ nm, indicating that both the as-prepared and melt-recrystallized carbon-coated ultrathin PE films exhibit the same crystalline structures. Moreover, the alignment of the (002) reflections along the drawing direction during film preparation tells us that the carbon-coated ultrathin PE films have also the same chain orientation before and after heat treatment, i.e., the PE molecular chains arranged in the film plane and parallel to the drawing direction. It should be pointed out that the electron diffraction pattern of the as-prepared PE film (Figure 1a) displays much more diffraction spots than its melt-recrystallized counterpart (Figure 1b). This is caused by different spatial arrangements of the PE crystals. For the as-prepared PE film, the coexistence of (110), (200), and (020) reflection spots in Figure 1a indicates a fiber orientation with their crystallographic *a*- and *b*-axes rotated randomly about the chain direction. On the contrary, the disappearance of (200) reflections and remarkable intensity decrease of the (110) reflections in Figure 1b indicate that the recrystallized PE film possesses a double orientation with the crystallographic *c*- and *b*-axes oriented in the film plane and the molecular chains arranged parallel to the drawing direction. This results from the thin film crystallization habit that the fastest growth direction, *b*-axis for PE, grows preferentially in the film plane.[18]

The electron diffraction results demonstrate that the chain orientation of a uniaxially oriented ultrathin PE film has been preserved by a vacuum-evaporated thin carbon layer during melt recrystallization. The spatial arrangement of the PE crystals has, however, changed during the melt recrystallization process. To see the morphological differences, the phase contrast AFM images of the carbon-coated ultrathin PE melt-drawn films before and after heat treatment are presented in Figure 2. The white arrows in the pictures represent the drawing direction of the films during preparation. It is clear that in both cases the PE films consist of oriented crystals. This again confirms that the carbon coating leads to an oriented recrystallization of the preoriented ultrathin PE films. With close inspection, different

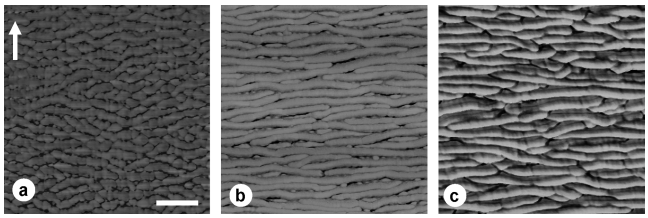

Figure 2. AFM images of the carbon-coated ultrathin PE melt-drawn films before and after heat treatment: (a) as-prepared PE thin film; (b) and (c) after melting at 150 °C for 10 min and then isothermal recrystallization for 2 h at 100 and 120 °C, respectively. The arrow represents the drawing direction of the films during preparation. Scale bar 200 nm.

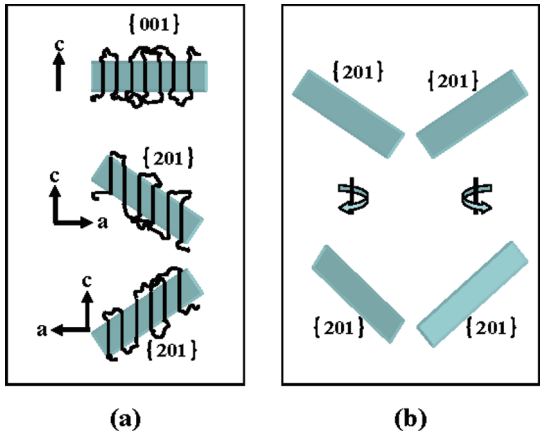

Figure 3. Sketches showing (a) the orientations of the PE lamellae with {001} and {201} fold surfaces and (b) their variation in the fiber orientation when the PE crystals rotated randomly around their *c*-axis.

morphological features of the PE films before and after heat treatment can be easily recognized. First, the average lamellar thickness decreases from ca. 38 nm (Figure 2a) to about 33 nm (Figure 2b) after heat treatment. It results from the change in crystallization conditions, i.e., crystallization of the as-prepared film at ca. 125 °C under stress and quiescent melt recrystallization of it at exactly 100 °C. This has been well explained by many researchers[19−22] and also been verified here by changing the recrystallization temperature. As shown in Figure 2c, when the melt recrystallization was performed at 120 °C, highly oriented lamellae with average thickness of ca. 36 nm were observed. Second, while the recrystallized film shows wider and relatively smoother lamellar structure with the lamellae arranged perpendicular to the drawing direction, the as-prepared PE film shows microcrystalline structures. This should originate from the higher nucleation density of the as-prepared PE film caused by stretching. Third, while the similar well-defined (002) reflections indicate the same chain orientation of the PE thin films before and after heat treatment, the AFM images show that the recrystallized PE ultrathin films presented in Figure 2b and c seem to have a better orientation than the as-prepared one. This is caused by different folding planes combined with different spatial arrangement of the PE crystals. As sketched in Figure 3a, when the fold surfaces are the {001} surfaces, lamellae with long axes perpendicular to the *c*-axis will be formed. On the other hand, if the fold surfaces are the {201} surfaces, lamellae with long axes 55.6° apart from the *c*-axis will be observed. Taking this into account, in the recrystallized PE ultrathin film, the PE lamellae with {001} surfaces along [010] growth direction are produced. This is revealed as long lamellae aligned perpendicular to the *c*-axis direction in the AFM images (Figure 2b and c) and results in the disappearance of (200) reflections in the electron diffraction pattern (Figure 1b). As for the as-prepared ultrathin PE film, considering that the PE crystallizes under stress at about 125 °C, which is close to the regime I to II transition temperature,[23] crystals with different fold surfaces, e.g., {001} and {201} fold surfaces, could present. Moreover, taking the fiber orientation of the as-prepared PE film into account, the rotation of *a*-axis around the *c*-axis makes the morphology even more complicated (Figure 3b). All these lead to an unparallel alignment of the chain direction and the normal direction of the lamellar fold surfaces.

To follow the oriented recrystallization process of the preoriented PE thin films, infrared spectroscopy was employed. Figure 4 shows the polarized infrared spectra of the carbon-coated ultrathin PE melt-drawn films before and after heat treatment in the CH_2 stretching vibration region. The spectra with electron vector perpendicular to the drawing direction of the film are indicated as 90°, while those with the electron vector parallel to the drawing direction of the film are indicated as 0°. It is obvious that in both cases the absorption intensity of the perpendicular polarization is much stronger than that of the parallel polarization. This demonstrates that both the original and the recrystallized PE films exhibit a similar orientation. This result is in good accord with the electron diffraction and reflects an oriented recrystallization of the ultrathin PE film. In IR analysis, the chain orientation status is usually characterized by infrared dichroic ratio (R) defined as $R = A_{\perp}/A_{\parallel}$, with $A_{\perp}$ and $A_{\parallel}$ reflecting the absorbance when the infrared beam was polarized perpendicular and parallel to the chain direction, respectively. From Figure 4, we found that the R value of 2918 cm^{-1} decreased evidently, from 6.35 for the original film to 4.47 for the recrystallized film, after melt recrystallization. This implies a reduction in chain orientation and seems to be in contradiction to the electron diffraction results. It rests actually

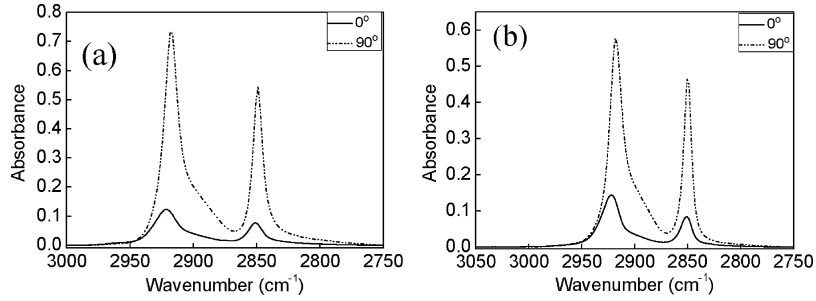

Figure 4. Polarized FTIR spectra of the carbon-coated ultrathin PE melt-drawn films (a) before and (b) after heat treatment in the CH_2 stretching vibration region. The spectra with electron vector perpendicular to the drawing direction are indicated as 90°, while those with the electron vector parallel to the drawing direction are indicated as 0°.

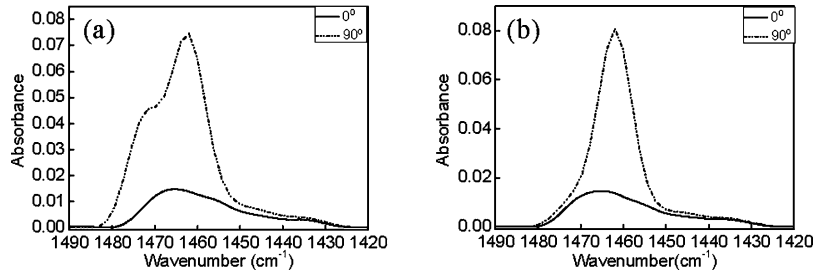

Figure 5. Polarized FTIR spectra of the carbon-coated ultrathin PE melt-drawn films (a) before and (b) after heat treatment in CH_2 bending vibration region.

on the facts that the band at 2918 cm^{-1} represents the total asymmetric and symmetric CH_2 stretching vibrations both in crystalline and amorphous phases,[24] while the electron diffraction reflects only the orientation of the crystalline phase. To distinguish the contribution of PE chains in crystalline phase from its amorphous counterpart, the polarized IR spectra of PE films in the CH_2 bending vibration region were analyzed.

Figure 5 shows the polarized FTIR spectra of carbon-coated ultrathin PE melt-drawn films in the CH_2 bending vibration region before and after heat treatment. It is reported that the doublet manifested in the infrared spectrum of PE corresponding to the CH_2 bending vibration at 1472 and 1462 cm^{-1} originates from a factor group splitting due to the close packing of two polymer chains in the unit cell of an orthorhombic lattice.[24] Furthermore, the vibration directions of these two bands at 1472 and 1462 cm^{-1} are both perpendicular to the chain skeleton axis but parallel to the crystallographic *a*- and *b*-axes of the unit cell, respectively. For the 1462 cm^{-1}, the *R* values are calculated to be 5.06 and 5.56 for the as-prepared and the melt-recrystallized PE films, respectively. This indicates a similar chain orientation of the PE crystals in both cases. Moreover, one can clearly see that the 1472 cm^{-1} band disappears completely after recrystallization. Considering that the 1472 cm^{-1} is parallel to the crystallographic *a*-axis, this result further suggests that in the melt-recrystallized PE film the *c*- and *b*-axes are preferentially oriented in the film plane with the molecular chains arranged parallel to the drawing direction.

RAIR spectroscopy is a powerful tool to study the orientation character of a thin film at a metal surface. Reflection on the metal surface results in an electrical field that is strongly elliptically polarized in RAIR measurement. With only a significant contribution of the component perpendicular to the film surface, the intensity of the corresponding band would become obviously stronger in the RAIR spectrum than that in the TIR spectrum. On the other hand, with a component parallel to the film surface, the intensity of the corresponding band would become weaker. Therefore, RAIR spectroscopy was utilized here to further confirm the above-mentioned crystal orientation. Figure 6 shows the RAIR spectra of the carbon-coated PE melt-drawn films before and after heat treatment in the CH_2 bending vibration region. The intensity changes of the bands at 1472 and 1462 cm^{-1} in the RAIR spectra can be clearly seen. The significant increase in intensity ratio of 1472 and 1462 cm^{-1} bands, namely, A_{1472}/A_{1462}, again confirms that the crystallographic *a*- and *b*-axes are preferentially aligned perpendicular to the film plane and in the film plane, respectively. These results are in good agreement with the electron diffraction results, indicating a good reliability of the IR spectroscopy on analysis of polymer chain organization. Therefore, it was used to study the mechanism of the oriented recrystallization behavior of carbon-coated PE-oriented thin films.

We previously suggested that the oriented recrystallization of preoriented polymer thin films is caused by the fixing effect

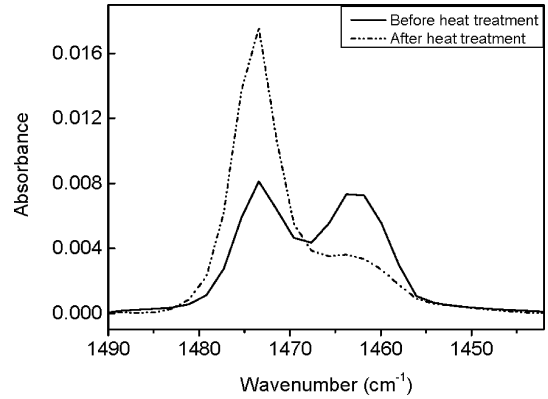

Figure 6. RAIR spectra of the carbon-coated ultrathin PE melt-drawn films before and after heat treatment in the CH_2 bending vibration region.

of the carbon layer on the surface monolayer of the oriented polymer film, which prevents the polymer chain stems in the crystalline phase from relaxation at high temperature. To find out the validity of this hypothesis, polarized FTIR spectra of three different PE melt-drawn films in the CH_2 stretching vibration region were recorded at 150 °C, above the melting point of PE. For the PE melt-drawn film with one surface carbon-coated, as shown in Figure 7a, one can find with close inspection that the absorption intensity with the infrared beam polarized perpendicular to the drawing direction is somewhat stronger than that parallel to the drawing direction. On the contrary, for the PE melt-drawn film without carbon coating, as shown in Figure 7b, the spectra are exactly the same, indicating the independence of the absorption with respect to the polarization direction of the infrared beam. This implies that there are indeed some PE chain stems are not relaxed at 150 °C, or at least not completely relaxed, in the carbon-coated PE film. Taking the tiny difference into account, one may suggest that this difference is caused by system error of the instrument. This is not the case since repeated experiments show always the same results. Moreover, it is reasonable to assume that the amount of the nonrelaxed chain segments should be increased if the oriented PE films are carbon-coated on both surfaces. As shown in Figure 7c, the difference between the spectra with the infrared beam polarized perpendicular and parallel to the drawing direction is indeed enhanced by both sides carbon coating. The corresponding difference spectrum of Figure 7c, present as part d of Figure 7, displays more clearly the absorption intensity difference.

The above experimental result demonstrates that the vacuum-evaporated carbon layer exhibits a fixing effect toward the surface monolayer PE, which prevents the PE chain stems in the surface monolayer from relaxation at high temperature. These preserved PE chain stems will act as nucleation sites and induce oriented recrystallization of the PE film. This fixing effect

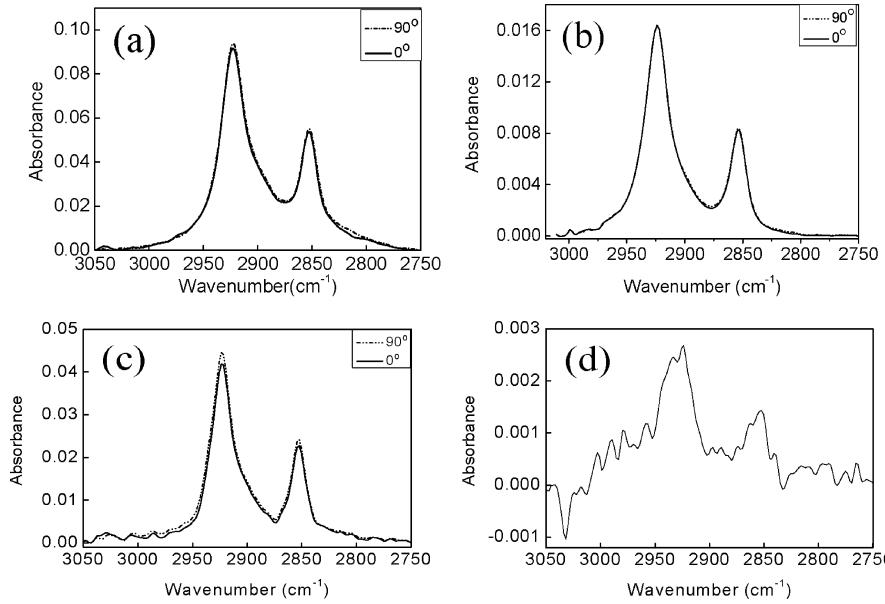

Figure 7. Polarized FTIR spectra of melt-drawn PE ultrathin films (a) with one surface carbon-coated, (b) without carbon coating, and (c) with both surfaces carbon-coated. The spectra were recorded at 150 °C in the CH_2 stretching vibration region. (d) Difference spectrum resulting from part c.

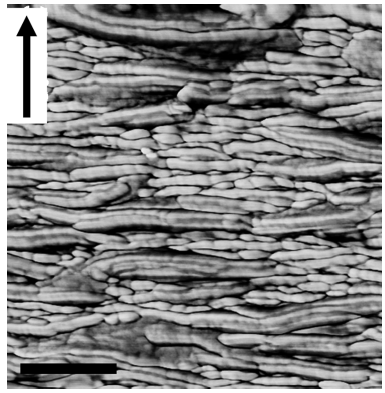

Figure 8. AFM image of a carbon-coated PE melt-drawn film, which has been heated to 350 °C for 3 min and subsequently cooled to room temperature at 10 °C/min. The arrow indicates the molecular chain direction, i.e., the drawing direction during sample preparation. Scale bar 500 nm.

is confirmed to survive at very high temperature, e.g., 350 °C (see Figure 8), and can promote an oriented crystallization of a PE film as thick as hundreds of nanometers, e.g., 500 nm. As for the origin of this fixing effect, one may suggest that carbon free radicals may be generated during vacuum evaporation and may have linked to the surface of PE film via covalent bonds. To confirm this, Raman spectra were recorded.

Figure 9a shows the Raman spectra of the as-prepared and carbon-coated PE melt-drawn films. For comparison, the Raman spectrum of a pure vacuum-evaporated carbon layer is presented in Figure 9b. One can clearly see the difference between the as-prepared and the carbon-coated PE films. For the carbon-coated PE film, except for a broad band contributed by the vacuum-evaporated carbon layer, there are four bands appearing at 1062, 1129, 1295, and 1416 cm^{-1}, while two bands disappeared at 1460 and 1440 cm^{-1}. Moreover, an intensity increase of the 1129 cm^{-1} band and an intensity decrease of the 1295 cm^{-1} band can be clearly seen. It was reported that the 1129 and 1295 cm^{-1} bands are associated with the C−C stretching and the CH_2 twisting modes, respectively.[25−27] Taking this into account, the inverse intensity changes of the 1129 and 1295 cm^{-1} bands demonstrate the formation of new C−C bonds. It is reasonable to assume that these newly formed C−C bonds connect the vacuum-evaporated carbon layer and the oriented PE film since no C−C bonds have been detected for pure carbon film. The mechanism of the newly formed C−C bonds is not clear now. Since there are not unsaturated chemical bonds in the PE, the only possibilities are the cleavage of the C−C and C−H bonds. Considering that the bond energy of the C−C is higher than that of the C−H bonds, the reaction of carbon radicals with the C−H bonds is speculated. A detailed study on the reaction mechanism will be performed.

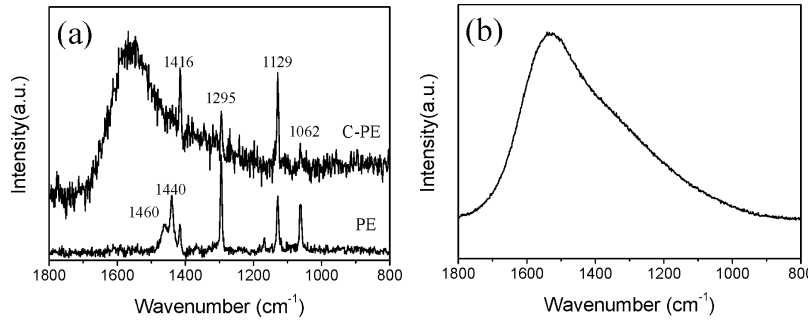

Figure 9. Raman spectra of (a) the as-prepared and carbon-coated melt-drawn PE films and (b) the vacuum-evaporated carbon film.

Conclusions

The melting and recrystallization behavior of carbon-coated ultrathin PE oriented films was studied by AFM, electron diffraction, infrared spectroscopy, and Raman spectroscopy. The electron diffraction results show that the molecular chain orientation of the preoriented PE ultrathin film is preserved by a layer of vacuum-evaporated carbon during melt recrystallization. While the as-prepared PE film exhibits a fiber orientation, the recrystallized PE film with carbon coating possesses a double orientation with *b*- and *c*-axes in the film plane and the *c*-axis along the drawing direction during film preparation. Reflection−absorption infrared spectroscopy result further confirms the double orientation of the melt-recrystallized PE thin film with a vacuum-evaporated carbon layer. AFM observations show that the as-prepared PE ultrathin film consists of microcrystallites with different fold surfaces, whereas the recrystallized PE film exhibits wider edge-on lamellae with {001} fold surfaces. Moreover, polarized infrared spectroscopy results demonstrate the existence of some oriented PE chain segments in the molten state of the carbon-coated PE ultrathin film, indicating the fixing effect of the carbon layer on the PE film. Raman spectroscopy result indicates that during carbon evaporation some new carbon−carbon bonds have been created between the vacuum-evaporated carbon layer and the preoriented PE film. These C−C bonds have prevented the relaxation of PE molecular chain stems in the surface monolayer at very high temperature. The nonrelaxed PE molecular chain stems in turn act as nucleation sites and induce the oriented recrystallization of the preoriented PE films.

Acknowledgment. The financial support of the National Natural Science Foundations of China (No. 50833006, 20634050, and 50973008) and the program of Introducing Talents of Discipline to Universities (B08003) is gratefully acknowledged.

References and Notes

(1) Paquette, J.; Vali, H.; Mucci, A. *Geochim. Cosmochim. Acta* **1996**, *60*, 4689–4700.
(2) Poorhaydari, K.; Ivey, D. G. *Mater. Char.* **2007**, *58*, 544–554.
(3) Sakai, H.; Matsumura, A.; Yokoyama, S.; Saji, T.; Abe, M. *J. Phys. Chem. B* **1999**, *103*, 10737–10740.
(4) Keller, A.; Bassett, D. C. *J. R. Micr. Soc.* **1960**, *79*, 243–261.
(5) Bassett, D. C.; Keller, A. *Philos. Mag.* **1961**, *6*, 345–358.
(6) Bassett, D. C. *Philos. Mag.* **1961**, *6*, 1053–1056.
(7) Lü, K.; Yang, D. *Macromol. Rapid Commun.* **2005**, *26*, 1159–1162.
(8) Taniguchi, N.; Kawaguchi, A. *Macromolecules* **2005**, *38*, 4761–4768.
(9) Wang, J.; Li, H.; Liu, J.; Duan, Y.; Jiang, S.; Yan, S. *J. Am. Chem. Soc.* **2003**, *125*, 1496–1497.
(10) Yan, S. *Macromolecules* **2003**, *36*, 339–345.
(11) Liu, J.; Li, H.; Duan, Y.; Jiang, S.; Miao, Z.; Wang, J.; Wang, D.; Yan, S. *Polymer* **2003**, *44*, 5423–5428.
(12) Yan, S.; Lieberwirth, I.; Katzenberg, F.; Petermann, J. *J. Macromol. Sci. B, Phys.* **2003**, *B42*, 641–652.
(13) Yan, S.; Katzenberg, F.; Petermann, J. *J. Polym. Sci., Part B: Polym. Phys.* **1999**, *37*, 1893–1898.
(14) Takahashi, Y. *Macromolecules* **2001**, *34*, 7836–7840.
(15) Tanaka, M.; Young, R. *J. Mater. Sci.* **2006**, *41*, 963–991.
(16) Zhang, J.; Sato, H.; Tsuji, H.; Noda, I.; Ozaki, Y. *Macromolecules* **2005**, *38*, 1822–1828.
(17) Petermann, J.; Gohil, R. *J. Mater. Sci. Lett.* **1979**, *14*, 2260–2264.
(18) Yang, D.; Thomas, E. *J. Mater. Sci.* **1984**, *19*, 2098–2110.
(19) Peterlin, A.; Ingram, P.; Kiho, H. *Makromol. Chem.* **1965**, *86*, 294–297.
(20) Bassette, D. C.; Dammont, F. R.; Salovey, R. *Polymer* **1964**, *5*, 579–588.
(21) Bassette, D. C. *Principles of Polymer Morphology*; Cambridge Unversity: Cambridge, 1981; *Chapter 5*.
(22) Wunderlich, B. *Macromolecular Physics*; Academic: New York, 1973; Vol. 1.
(23) Wagner, J.; Philiphs, P. J. *Polymer* **2001**, *42*, 8999–9013.
(24) Yan, C.; Zhang, J.; Shen, D.; Yan, S. *Chin. Sci. Bull.* **2006**, *51*, 2844–2850.
(25) Strobl, G.; Hagedorn, W. *J. Polym. Sci., Part B: Polym. Phys.* **1978**, *16*, 1181–1193.
(26) Tarazona, A.; Koglin, E.; Coussens, B.; Meier, R. *J. Vib. Spectrosc.* **1997**, *14*, 159–170.
(27) Sato, H.; Shimoyama, M.; Kamiya, T.; Amari, T.; Scaronascaronic, S.; Ninomiya, T.; Siesler, H. W.; Ozaki, Y. *J. Appl. Polym. Sci.* **2002**, *86*, 443–448.

JP106995F